HHS Public Access

Author manuscript

Gastroenterology. Author manuscript; available in PMC 2023 November 01.

Published in final edited form as:

Gastroenterology. 2022 November ; 163(5): 1281–1293.e1. doi:10.1053/j.gastro.2022.06.058.

Acetyl-coA Synthetase 2 potentiates macropinocytosis and muscle wasting through metabolic reprogramming in pancreatic cancer

Zhijun Zhou[1,2,†], **Yu Ren**[1,2,†], **Jingxuan Yang**[1,2,†], **Mingyang Liu**[1,2,†], **Xiuhui Shi**[1,2,†], **Wenyi Luo**[3], **Kar-Ming Fung**[3], **Chao Xu**[4], **Michael S. Bronze**[1], **Yuqing Zhang**[1,2,*], **Courtney W. Houchen**[1,*], **Min Li**[1,2,*]

[1]Department of Medicine, the University of Oklahoma Health Sciences Center, Oklahoma City, Oklahoma

[2]Department of Surgery, the University of Oklahoma Health Sciences Center, Oklahoma City, Oklahoma

[3]Department of Pathology, the University of Oklahoma Health Sciences Center, Oklahoma City, Oklahoma

[4]Department of Biostatistics and Epidemiology, Hudson College of Public Health, the University of Oklahoma Health Sciences Center, Oklahoma City, Oklahoma

Abstract

BACKGROUND & AIMS: Rapid deconditioning, also called cachexia, and metabolic reprogramming are two hallmarks of pancreatic cancer. ACSS2 is an acetyl-coA synthetase that contributes to lipid synthesis and epigenetic reprogramming. However, the role of ACSS2 on the non-selective macropinocytosis and cancer cachexia in pancreatic cancer remains elusive. In this study, we demonstrate that ACSS2 potentiates macropinocytosis and muscle wasting through metabolic reprogramming in pancreatic cancer.

[*]Address correspondence to: Min Li, PhD, Department of Medicine, Department of Surgery, The University of Oklahoma Health Sciences Center, 975 NE 10th Street, BRC 1262A, Oklahoma City, OK 73104, Tel: (405) 271-6145, Fax: (405) 271-1476, Min-Li@ouhsc.edu, Courtney W. Houchen, MD, Department of Medicine, The University of Oklahoma Health Sciences Center, 800 Stanton L. Young Blvd, Oklahoma City, OK 73104, Phone: 405-271-8001, ext. 54288; Courtney-Houchen@ouhsc.edu, Yuqing Zhang, PhD, Department of Medicine, The University of Oklahoma Health Sciences Center, 975 NE 10th Street, BRC 1215A, Oklahoma City, OK 73104, Phone: 405-271-8001, ext. 32523; Yuqing-Zhang@ouhsc.edu.

[†]Equal contributions.

Author contributions

Study concept and design: Zhijun Zhou, Yu Ren, Jingxuan Yang, Mingyang Liu, Yuqing Zhang, and Min Li. Acquisition of data: Zhijun Zhou, Yu Ren, Jingxuan Yang, Mingyang Liu and Xiuhui Shi. Analysis and interpretation of data: Zhijun Zhou, Yu Ren, Jingxuan Yang, Mingyang Liu, Xiuhui Shi, Yuqing Zhang, Wenyi Luo, Kar-Ming Fung, Chao Xu, Michael S. Bronze, Courtney W. Houchen and Min Li. Drafting the manuscript and critical revision: Zhijun Zhou, Yu Ren, Jingxuan Yang, Mingyang Liu, Yuqing Zhang, Michael S. Bronze, Courtney W. Houchen, and Min Li. All the authors have approved the final version of the paper.

Conflict of interest

Courtney W. Houchen has ownership interest in COARE Holdings Inc. Other authors declare no conflict of interest.

METHODS: Clinical significance of ACSS2 was analyzed using human pancreatic cancer patient samples. ACSS2 knockout cells were established utilizing CRISPR-Cas9 system. Single-cell RNA sequencing data from genetically engineered mouse models was analyzed. Macropinocytotic index was evaluated by dextran uptake assay. ChIP assay was performed to validate transcriptional activation. ACSS2 mediated tumor progression and muscle wasting were examined in orthotopic xenograft models.

RESULTS: Metabolic stress induced ACSS2 expression, which is associated with worse prognosis in pancreatic cancer. ACSS2 knockout significantly suppressed cell proliferation in 2D and 3D models. Macropinocytosis associated genes are upregulated in tumor tissues and are correlated to worse prognosis. ACSS2 knockout inhibited macropinocytosis. We identified ZIP4 as a downstream target of ACSS2, and knockdown of ZIP4 reversed ACSS2 induced macropinocytosis. ACSS2 upregulated ZIP4 through ETV4 mediated transcriptional activation. ZIP4 induces macropinocytosis through CREB activated SDC1 and DNM2. Meanwhile, ZIP4 drives muscle wasting and cachexia via GSK3β mediated secretion of TRAIL. ACSS2 knockout attenuated muscle wasting and extended survival in orthotopic mouse models.

CONCLUSIONS: ACSS2-mediated metabolic reprogramming activates ZIP4 pathway, and promotes macropinocytosis via SDC1/DNM2 and drives muscle wasting through GSK3β/TRAIL axis, which potentially provides additional nutrients for macropinocytosis in pancreatic cancer.

Lay summary

ACSS2 promotes macropinocytosis and muscle wasting through ETV4/ZIP4 mediated metabolic reprogramming, which provides additional nutrients to support tumor growth in pancreatic cancer.

Graphical Abstract

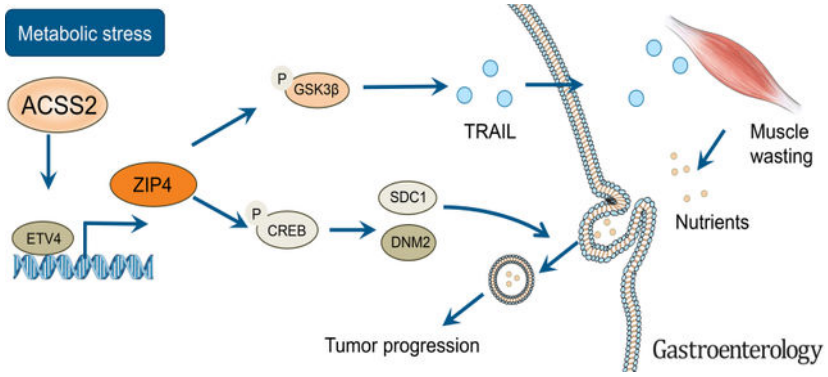

Keywords

Cachexia; Macropinocytosis; Metabolic Stress; Muscle Wasting

Introduction

Rapid deconditioning, also known as cancer cachexia, is a systemic dysfunction characterized by uncontrollable body weight loss independent of nutritional supplement.[1, 2] Muscle wasting, adipose loss and loss of appetite (anorexia) are prevalent in those patients.

Cachexia is associated with multi-organ dysfunction and increased mortality.[1, 3] Currently, no effective treatment options have been approved to reverse or ameliorate cancer cachexia.[4] Novel therapeutic targets and treatment strategies are urgently needed. Pancreatic cancer has the highest prevalence of cachexia among all cancer types, highlighting its unique pathological alterations for the development of cachexia.[1, 5]

Pancreatic cancer is characterized with desmoplasia, which created a hypoxic, acidic and nutrient deficient microenvironment compared to adjacent benign pancreas tissue.[6, 7] However, the mechanism of pancreatic cancer cells surviving in this nutrient deficiency remains elusive. Cancer cells develop multiple ways to overcome the metabolic stress induced by the hazard tumor microenvironment, such as increasing lipogenesis and nutrient uptake. Oncogenic RAS mutant tumor cells depend on protein scavenging to maintain tumor fitness in the nutrient deficient microenvironment, a process known as macropinocytosis.[8] Since most pancreatic cancer had KRAS mutation, macropinocytosis represents a critical source of amino acid supply for this devastating disease. Nonetheless, how pancreatic cancer cells coordinate between cachexia and macropinocytosis remains poorly defined.

Acyl-CoA Synthetase Short-Chain Family Member 2 (ACSS2) is an enzyme responsible for converting acetate into acetyl-CoA, which contributes to energy production and lipogenesis. It has been reported that ACSS2 helps tumor cells survive metabolic stress by reprogramming metabolic profiles in several tumor types, such as breast cancer and glioblastoma.[9, 10] Acidic microenvironment can induce ACSS2 expression via sterol regulatory element-binding proteins (SREBPs) in pancreatic cancer.[11] PanIN lesions and pancreatic cancer tissue also showed high expression of ACSS2.[12] Nevertheless, the role of ACSS2 on regulating metabolic stress and cancer cachexia in pancreatic cancer is unknown.

In this study, we found that metabolic stress can induce ACSS2 expression. Meanwhile, ACSS2 is upregulated in pancreatic cancer tissues, especially at the regions where tumor cells suffer from metabolic stress, such as the necrotic area. ACSS2 promotes macropinocytosis to maintain the supply of amino acids for tumor growth. ACSS2 upregulates macropinocytosis in an ETV4/ZIP4 dependent manner via SDC1 and DNM2. Furthermore, ZIP4 promotes muscle wasting through GSK3β B/TRAIL axis, resulting in cancer cachexia, which potentially provides nutrients to maintain tumor fitness. ACSS2 dominates the metabolic reprogramming by orchestrating macropinocytosis and muscle wasting to support tumor progression in pancreatic cancer. Targeting ACSS2 holds the promise for retarding the development of cancer cachexia in pancreatic cancer.

Materials and Methods

Cell Lines and Plasmids

Pancreatic cancer cell lines and C2C12 cells were obtained from American Type Culture Collection (ATCC, Rockville, MD), and were maintained in RPMI 1640 Medium or Iscove's Modified Dulbecco's Medium or Dulbecco's Modified Eagle Medium supplemented with 10% fetal bovine serum. All cell lines have been authenticated and evaluated as mycoplasma free. hACSS2 plasmid (EX-Z9293-Lv217) and the empty control vector (EX-NEG-Lv217) were purchased from Genecopoeia (Rockville, MD). The

eSpCas9(1.1) (Plasmid #71814), lenti sgRNA (MS2)_puro optimized backbone (Plasmid #73797), pLX_TRC311 (Plasmid #113668), pLX_TRC311 ETV4-L (Plasmid #74982) were obtained from Addgene.

CRISPR-Cas9

ACSS2 knockout cell lines were established using the CRISPR-Cas9 system.[13] Cas9 overexpression cell lines were established with the eSpCas9(1.1) (Plasmid #71814, Addgene). The guide RNA oligonucleotides that target ACSS2 were cloned into the sgRNA MS2 backbone plasmid (Plasmid #73797) using the Gibson Assembly (New England Biolabs).[14] The plasmids were collected with Plasmid DNA Maxiprep Kit (Invitrogen) and validated by sequencing. The plasmids were then introduced into the Cas9 overexpression cell lines. Mono-colonies of ACSS2 knockout cells were selected.

Chromatin Immunoprecipitation

Chromatin Immunoprecipitation was performed using the MAGnify Chromatin Immunoprecipitation System (Invitrogen) according the manufacturer's instruction. Briefly, cell pellets were crosslinked with formaldehyde, followed by lysing the cells and shearing the chromatin, which was then diluted and incubated with antibody-incorporated beads. The chromatin was washed, followed by reverse crosslinking and DNA purification. The purified DNA was then used for polymerase chain reaction.

Construction of Stable Cell Lines

Stable cell lines were constructed as previously described.[15, 16] Briefly, plasmids were amplified in Stbl3 competent E. coli cells and then collected by Plasmid DNA Maxiprep Kit (Invitrogen). Plasmids of interest, together with psPAX2 (#12260, Addgene) and VSV-G (#8454, Addgene) plasmids were transfected into 293Ta cells by lipofectamine 3000 (#L3000015, Invitrogen). After 48–72 hours, the supernatant was collected and filtered for the transfection of cells. The stable cells were selected with puromycin followed by single colony isolation.

3D Spheroid Model

The 3D spheroid model was constructed as previously described.[15, 16] Briefly, tumor cells were resuspended in culture medium with 0.24% methylcellulose and seeded as 20 μL droplets in the inner lid of 10 cm dish, which was filled with 10 mL phosphate buffer solution. The spheroids were allowed to grow in 5% CO_2 at 37°C. Images were taken at different time points to monitor the size of the spheroids.

Western Blot Analysis

Western blot was performed as previously described.[17] Cell lysates were loaded into sodium dodecyl sulfate–polyacrylamide gel for electrophoresis. After the electrophoresis, the protein was transferred onto nitrocellulose membrane and blocked in 5% skim milk at room temperature for 1 hour, followed by the incubation with desirable antibodies against ZIP4 (Proteintech, 1:2000), ACSS2 (Santa Cruz Biotechnology, 1:1000), ACTB (Proteintech, 1:10000), MuRF1 (R&D, 1:500), Atrogin-1 (ECM Biosciences, 1:1000), MHC (University

of Iowa, 1:1000), SDC1 (Proteintech, 1:1000), p- GSK3β (CST, 1:1000), total- GSK3β (CST, 1:1000), p-CREB (CST, 1:1000), total-CREB (CST, 1:1000), ETV4 (Aviva Systems Biology, 1:1000), or mouse ZIP4 (R&D, 1:1000) at 4°C overnight. Then, the membrane was washed with Tris-Buffered Saline buffer with 0.1% Tween 20, followed by the incubation of IRDye secondary antibodies (1:10,000) at room temperature for 2 hours. The results were examined by Odyssey Imager (LI-COR).

EdU Incorporation Assay

The EdU incorporation assay was performed using the Click-iT™ EdU Cell Proliferation Kit (#C10339, ThermoFisher) following the manufacturer's instructions. Tumor cells were seeded on the chamber slides and allowed to grow overnight. Cells were then cultured with medium containing EdU (10uM) for 3–4 hours and fixed by 3.7% formaldehyde in PBS for 15 minutes at room temperature, followed by permeabilization with 0.5% Triton X-100 before incubated with Click-iT® reaction cocktail at room temperature for 30 minutes, followed by DNA staining with Hoechst at room temperature for 20–30 minutes. The images were captured by an Olympus Fluorescence Microscope.

Quantitative Reverse Transcription PCR

RNA was purified by PureLink™ RNA Mini Kit (#12183025, ThermoFisher) and cDNA was obtained using cDNA Reverse Transcription Kit (#4368814, ThermoFisher) following the manufacturer's instructions. PowerUp™ SYBR™ Green Master Mix (#4367659, ThermoFisher) was utilized for quantitative PCR by LightCycler® 96 Instrument (Roche). Primers used for RT-qPCR are listed in Supplementary Table S1.

MTT Assay

Cells were seeded in 96-well plate at desirable density and allowed to grow overnight. Culture medium was then removed and each well was added with alamarBlueTM (Bio-Rad) and cultured at 37°C for 2 hours according to manufacturer's instructions. Results were examined with a microplate reader (Bio-Tek).

Pancreatic Cancer Orthotopic Xenograft Mouse Model

Athymic nude male mice of 5–6 weeks old were used for this study. All mice were taken care of according to the study protocol approved by the Animal Welfare Committee at OUHSC. ASPC-Cas9, ASPC-ACSS2-KO, CFPAC-Cas9, CFPAC-ACSS2-KO stable cell lines were used to establish the orthotopic xenograft pancreatic cancer model. Briefly, tumor cells were trypsinized and resuspended in RPMI-1640 or Iscove's Modified Dulbecco's Medium at a density of 6×10^7 cells/mL. The mice were maintained anesthesia with Isoflurane during surgery. Surgical aseptic technique was applied for the construction of the model. Each mouse was injected with 50 μL cell suspension containing 3×10^6 pancreatic cancer cells into the pancreas. The wound was sutured with a Vicryl Suture 4–0 (Ethicon). The mice were sacrificed after 5–6 weeks for tissue collection. For survival analysis, mice were carefully monitored and euthanized when they were moribund or reached the endpoint of the study protocol.

Dextran Uptake Assay

Dextran uptake assay was performed to evaluate macropinocytosis.[18] Briefly, cells were seeded on chamber slides at desirable density and allowed to grow for 24 to 48 hours followed by the starvation in culture medium with 0.1% FBS for 24 hours. Cells were treated with 1mg/mL Dextran (#D1818, ThermoFisher) at 37 °C for 1 hour, followed by PBS wash and fixation with 3.7% formaldehyde for 30 minutes at room temperature. After nuclei staining with Hoechst at room temperature for 20–30 minutes, images were captured by an Olympus Fluorescence Microscope and analyzed by ImageJ (NIH).

Immunohistochemistry

Tissues were fixed in formalin and embedded in paraffin, followed by sectioning into 4-μm thickness slides. Staining was performed as previously described. Briefly, the slides were deparaffinized followed by antigen retrieval in citrate-based solution. The endogenous peroxidase was quenched in 3% H_2O_2 at room temperature for 10 minutes, followed by blocking with 2.5% horse serum. The sections were then incubated in primary antibody at 4 °C overnight, followed by incubation with HRP Horse Anti-Rabbit IgG antibody for 30 minutes and DAB substrate for around 1 minute at room temperature. Hematoxylin QS was used for nuclear staining. The slides were then dehydrated, mounted and evaluated under a phase-contrast microscope. The cross-sectional areas of muscle fibers were analyzed in Image J (NIH).

Statistical Analysis

All of the analyses were performed in R (4.1.1) and Prism (GraphPad 9.0). The unpaired two-tailed Student's test was applied for two-group comparison unless otherwise indicated. Survival data was analyzed using the log-rank test. Statistical significance was determined by P value (*P<0.05, **P<0.01, *** P<0.001, **** P<0.0001).

Results

Metabolic Stress Induces ACSS2 Expression, which Promotes Cell Proliferation

The microenvironment of pancreatic cancer is characterized with metabolic stress induced by nutrient deficiency and hypoxia. We found that nutrient deficiency increased ACSS2 expression in pancreatic cancer cells (Figure 1A and Supplementary Figure 1A). Pancreatic cancer tissues also showed higher level of ACSS2 expression compared to normal pancreas tissues (Figure 1B and Supplementary Figure 1B). Higher ACSS2 expression is associated with worse overall survival in patients with pancreatic cancer (Supplementary Figure 1C). To further examine the function of ACSS2, we established the ACSS2 knockout and overexpression pancreatic cancer cell lines, including AsPC-1 (cachectic) and CFPAC-1 (non-cachectic) cells (Supplementary Figure 1D and E). EdU incorporation assay showed that DNA synthesis rate was decreased in ACSS2 knockout cells and increased in ACSS2 overexpressed cells (Figure 1C). Knockdown of mouse ACSS2 in *Kras*^{G12D} *Trp53*^{R172H}*Pdx1-Cre* (KPC) cells also decreased DNA synthesis (Figure 1D and Supplementary Figure 1F). We found that ACSS2 knockout decreased cell proliferation and colony formation, while ACSS2 overexpression increased cell proliferation in human

pancreatic cancer cells (Figure 1E and F, Supplementary Figure 1G and H). Transient and stable knockdown of ACSS2 in pancreatic cancer cells also resulted in decreased cell proliferation (Supplementary Figure 1I). Furthermore, we established the 3D spheroid model and found that ACSS2 knockout decreased the size of spheroids, while ACSS2 overexpression increased the size of spheroids (Figure 1G and H, Supplementary Figure 1J). These results indicate that metabolic stress induced ACSS2 expression and ACSS2 knockout suppressed cell proliferation in pancreatic cancer.

ACSS2 Upregulates Macropinocytosis in Pancreatic Cancer Progression

Emerging evidence showed that metabolic stress can upregulate macropinocytosis, a non-selective protein scavenging process, which grants tumor cells growth advantage in nutrient limitation. We analyzed single-cell RNA-seq data (GSE125588) to evaluate the expression of macropinocytosis associated genes (*Sdc1, Dnm2, Snx33, Pycard, Lrrc16a, Appl2*) in the pancreas of normal mice as well as several genetically engineered mouse models (GEMMs) of pancreatic cancer, including early-stage (40 days) and late-stage (60 days) *KIC* and *KPC* mouse models. We found that the level of macropinocytosis associated genes were increased during tumor progression (Supplementary Figure 2 and 3). We then evaluated the expression of those genes in human pancreatic cancer tissues and found that the expression of these macropinocytosis associated genes were increased in pancreatic tumor tissues compared to adjacent benign tissues (Figure 2A and Supplementary Figure 4A–C). ACSS2 expression is positively associated with macropinocytosis gene expression in cancer cells in Cancer Cell Line Encyclopedia (CCLE) database and in patients with pancreatic cancer (Supplementary Figure 4D). The upregulation of these genes was associated with worse overall survival in patients with pancreatic cancer (Supplementary Figure 4E–G). This prompted us to investigate whether ACSS2 promotes pancreatic cancer progression by upregulating macropinocytosis. We further examined the uptake of dextran (70kDa) in AsPC-1 and CFPAC-1 cells (Figure 2B), and found that ACSS2 knockout decreased dextran uptake, while ACSS2 overexpression increased dextran uptake. Furthermore, knockdown of ACSS2 expression decreased dextran uptake in KPC cells (Figure 2C). Overexpression of ACSS2 increased the mRNA levels of several macropinocytosis associated genes, including SDC1, DNM2, SNX33, PYCARD, LRRC16A and APPL2 in AsPC-1 and CFPAC-1 cells. ACSS2 knockout did not affect the expression of LRRC16A in AsPC-1 cells and SNX33 in CFPAC-1 cells, respectively (Figure 2D and E). APPL2 and PYCARD genes was not upregulated in tumor tissues compared with the benign tissues. Therefore, we focused on SDC1 and DNM2 in the subsequent study. To examine the impact of metabolic stress on SDC1 and DNM2, pancreatic cancer cells were cultured in normal condition (indicated as 10% FBS hereafter) or nutrient stress condition (indicated as 1% FBS hereafter). We found that nutrient stress increased the expression of ACSS2, SDC1 and DNM2. Knockout of ACSS2 decreased the expression of SDC1 and DNM2 (Figure 2F and G, Supplementary Figure 5A–D). Overexpression of ACSS2 upregulates SDC1 and DNM2 (Supplementary Figure 5E–G). These findings suggest that metabolic stress induces ACSS2, which upregulates macropinocytosis through SDC1 and DNM2.

ACSS2 Promotes Macropinocytosis through ZIP4

To identify the downstream target of ACSS2 that mediates macropinocytosis, we analyzed the transcriptomic data of pancreatic cancer tissues in TCGA dataset. By comparing the differentially expressed genes between ACSS2-low and ACSS2-high tumors, we identified a subset of genes that are positively correlated with ACSS2 expression in pancreatic cancer (Supplementary Figure 6A). Among these candidates, we are particularly interested in ZIP4, a zinc importer that plays critical roles in cancer metastasis, chemoresistance and cachexia in pancreatic cancer. We found that ZIP4 expression is higher in pancreatic cancer tissues compared to benign pancreas tissues (Supplementary Figure 6B). ZIP4 expression is positively correlated to ACSS2 expression in multiple pancreatic cancer cohorts (GSE16515, GSE28735, TCGA) and in cancer cell lines in CCLE dataset (Figure 3A–C and Supplementary Figure 6C and D). ACSS2 knockout decreased ZIP4 expression, while ACSS2 overexpression upregulated ZIP4 expression in human pancreatic cancer cell lines (Figure 3D–F, Supplementary Figure 6E–G). We also validated these findings in KPC cell lines (Figure 3G and Supplementary Figure 6H). Then, we evaluated whether ACSS2 promotes macropinocytosis through ZIP4. We knocked down ZIP4 expression in ACSS2 overexpressed pancreatic cancer cells and found that it decreased the expression of macropinocytosis associated gene profiles (Supplementary Figure 6I). These findings prompted us to evaluate whether ACSS2 increased cell proliferation through ZIP4 mediated macropinocytosis. ZIP4 knockdown in ACSS2 overexpressed pancreatic cancer cells suppressed dextran uptake in normal condition and stress condition (Figure 3H and I). Meanwhile, knockdown of ZIP4 reversed the upregulated DNA synthesis rate induced by ACSS2 overexpression (Figure 3J and K). Dependency score analysis showed that knockout of ZIP4 suppressed proliferation of pancreatic cancer cells (Supplementary Figure 6J). ZIP4 in combination with macropinocytosis associated genes, such as SDC1 and DNM2 can better stratify patients with different prognosis (Supplementary Figure 6K and L). Together, these results demonstrate ACSS2 promotes macropinocytosis through ZIP4.

ACSS2 Upregulates ZIP4 through ETV4

To identify the putative transcription factors that mediates ACSS2 upregulated ZIP4 expression, we analyzed the pancreatic cancer tissue samples in the TCGA database and found 6450 ZIP4-correlated genes ($P<0.001$), 4530 ACSS2 correlated genes ($P<0.001$). We also analyzed the JASPAR database and the UCSC Genome Browser and identified 47 potential transcription factors for ZIP4. Then, we merged these gene clusters and got the consensus genes that serve as the potential transcription factors for ZIP4, including ETV4, MEF2C, IKZF1, KLF9, ZNF135, ZBTB6, KLF16, SMAD2, MEF2A, GATA2, KLF5, ZNF148, and GLI3. Among these transcription factors, ETV4, KLF16 and KLF5 are positively correlated with ACSS2 (Figure 4A). We are interested in ETV4 and KLF16, which play critical roles in promoting pancreatic cancer progression. Knockdown of ACSS2 decreased the mRNA level of ETV4 and KLF16 (Figure 4B). Then, we examined the expression level of these two transcription factors in pancreatic cancer tissues and normal tissues. We found that only ETV4 but not KLF16 was increased in pancreatic cancer tissues compared with normal pancreas tissues (Supplementary Figure 7A–F). ETV4 is associated with ACSS2 and ZIP4 expression in patients' tumor tissues (Supplementary Figure 7G and H). We found that ETV4 overexpression can increase the mRNA level of ZIP4 in pancreatic

cancer cells (Figure 4C and Supplementary Figure 7I). To further validate that ETV4 can transcriptionally activate ZIP4, we analyzed the promoter region of ZIP4 and identified two potential binding motifs of ETV4. We performed chromatin immunoprecipitation (ChIP) using ETV4 antibody and found that ETV4 can bind to the promoter region of ZIP4 (Figure 4D and Supplementary Figure 7J). Overexpression of ACSS2 upregulated ETV4. We further validated that loss of ACSS2 reduced metabolic stress induced upregulation of ETV4 (Figure 4E and F, Supplementary 7K and L). To further investigate the role of ETV4 in this signaling axis, we examined the histone H3 lysine 27 acetylation (H3K27ac) on the enhancer or promoter region, which can activate gene expression.[19] We found that ACSS2 can directly regulates histone acetylation.[20] To explore whether ACSS2 upregulates ETV4 through H3K27ac modification on the promoter region of ETV4, we performed ChIP-PCR assay and demonstrated that ACSS2 increases H3K27ac modification on the promoter region of ETV4 and when ACSS2 was knocked out, the level of H3K27ac modification on the promoter region of ETV4 was decreased (Supplementary Figure 7M). These findings demonstrate that ACSS2 upregulates ZIP4 through ETV4, via H3K27ac modification.

ACSS2 Promotes Macropinocytosis through ZIP4/CREB Pathway

ACSS2 induced the expression of ZIP4 and phosphorylation of GSK3β and CREB, while knockout of ACSS2 decreased ZIP4 expression and phosphorylation of GSK3β and CREB (Figure 4E and F, Supplementary Figure 7K and L). Knockdown of ETV4 downregulated the phosphorylation of GSK3β and CREB in AsPC-1 cells but not in CFPAC-1 cells (Figure 4G and Supplementary Figure 7N and O). Previously we have shown that ZIP4 promotes pancreatic cancer progression by activating CREB.[21] SDC1 is a downstream target of CREB.[22] To examine whether CREB can transcriptionally activate SDC1 in pancreatic cancer, we performed ChIP assay and validated that CREB can bind to the promoter region of SDC1 in pancreatic cancer cells (Figure 4H). Overexpression of ETV4 promoted cell proliferation in pancreatic cancer (Figure 4I). Knockdown of ETV4, SDC1 and DNM2 decreased macropinocytosis and cell proliferation (Supplementary Figure 8A and B). Taken together, these results indicate that ACSS2 promotes macropinocytosis by upregulating macropinocytosis associated genes, such as SDC1 and DNM2, which are activated through ZIP4/CREB pathway.

ACSS2 Knockout Suppresses Tumor Growth in Orthotopic Xenograft Mouse Models

To validate the role of ACSS2 *in vivo*, we established the orthotopic xenograft mouse models using AsPC-Cas9, AsPC-ACSS2-KO, CFPAC-Cas9, CFPAC-ACSS2-KO cells (Figure 5A and B, Supplementary Figure 9A). ACSS2 knockout suppressed tumor growth in both models. ACSS2 knockout in AsPC-1 cells significantly decreased abdominal dissemination, and extended overall survival of the mice (55 vs 44 days, P = 0.0465, Figure 5C and D). In CFPAC-1 cells which prefer to disseminate to the wound of incision, ACSS2 knockout dramatically suppressed tumor grow on wound (Supplementary Figure 9B). ACSS2 expression is high in the area with metabolic stress, such as necrosis (Figure 5E and Supplementary Figure 9C). ACSS2 knockout tumors showed decreased expression of Ki-67, ZIP4 and macropinocytosis associated genes (SDC1 and DNM2) (Figure 5F and G, Supplementary 9D and E). These data demonstrate that ACSS2 knockout suppresses tumor

growth in mouse model, partially through decreasing the expression of macropinocytosis associated genes and macropinocytosis of tumor cells.

ACSS2 Promotes Muscle Wasting through GSK3β/TRAIL Pathway

We found that mice xenografted with AsPC-ACSS2-KO tumors showed attenuated weight loss compared to AsPC-Cas9 tumors (Supplementary Figure 10A). This finding prompted us to evaluate the muscle wasting and adipose loss in these mice. We found that ACSS2 knockout attenuated muscle wasting and adipose loss (Figure 6A and B, Supplementary Figure 10B–D). Since a majority of cancer cachexia induced deaths were attributed to muscle wasting, we focused on the role of ACSS2 on muscle wasting. ACSS2 knockout attenuated the decrease of muscle grip strength (Figure 6C). We evaluated the cross-sectional area of mouse tibialis anterior (TA) muscle and gastrocnemius (GAS) muscle, and found that ACSS2 knockout group had larger cross-sectional area of muscle fibers (Figure 6D–F and Supplementary Figure 10E–G). ACSS2 knockout decreased the expression of muscle wasting markers Atrogin-1 and MuRF1 in mouse muscle tissues (Figure 6G). To explore the underlying mechanism, we established the *in vitro* muscle differentiation model using the myoblasts C2C12 cells. C2C12 cells were differentiated into myotubes and treated with conditioned medium collected from AsPC-Cas9 or AsPC-ACSS2-KO cells. We found that conditioned medium from ACSS2 knockout cells decreased phosphorylation of p38 and suppressed the expression of MuRF-1 and Atrogin-1 in myotubes (Figure 6H and I, Supplementary Figure 10H). Meanwhile, it attenuated the decrease of Myosin Heavy Chain (MHC) in myotubes (Figure 6J). These results indicate that ACSS2 knockout reduces muscle wasting *in vivo* and *in vitro*.

Next, we explored the mechanism of ACSS2 induced muscle wasting. We examined the expression of several pro-cachexia factors including TRAIL (TNFSF10), TGF-β, IL-1A and IL-1B. We found that ACSS2 knockout decreased the transcription of these pro-cachexia factors (Figure 6K and L). Meanwhile, we also examined the levels of several anti-cachexia factors, including FGF2 and IL-15 (Supplementary Figure 10J–K). We found that ACSS2 knockout increased the transcription of these anti-cachexia factors in the pancreatic cancer cells. Overexpression of ACSS2 increased TRAIL and decreased FGF2 mRNA level (Figure 6M and Supplementary Figure 10L). We further validated that ACSS2 upregulated the expression of TRAIL in AsPC-1 cells (cachectic cell line) but not in CFPAC-1 cells (non-cachectic cell line) (Figure 6N and Supplementary Figure 10M). ZIP4 knockdown reversed ACSS2 upregulated TRAIL expression and reversed ACSS2 induced muscle wasting (Figure 6O and Supplementary Figure 10N). TRAIL expression is lower in ACSS2 knockout tumor tissues (Supplementary Figure 10P). TRAIL is associated with worse overall survival in patients with pancreatic cancer (median OS: 17.0 vs 24.3 months, Supplementary Figure 10Q). Combination of TRAIL and ZIP4 may stratify patients with different prognoses (Figure 6P). Those with simultaneously high expression of TRAIL and ZIP4 had worst prognoses (median OS: 15.1 months), while those with simultaneously low expression of TRAIL and ZIP4 had best prognoses (median OS: 43.8 months).

Discussion

Our current study found that knockout of ACSS2 can suppress cell proliferation in 2D and 3D models *in vitro* and suppress tumor metastasis and cachexia *in vivo*. Mechanism study showed that ACSS2 promotes macropinocytosis of tumor cells via ETV4/ZIP4/CREB mediated reprogramming of macropinocytosis associated genes. Meanwhile, ZIP4 promotes muscle wasting through GSK3β/TRAIL axis, which in turn provides additional nutrient to maintain tumor fitness. ACSS2 can induce autophagy of tumor cells under nutritional stress, such as glucose deprivation, via regulating histone acetylation in glioblastoma.[23] Meanwhile, previous studies showed that knockout of ACSS2 can suppress tumorigenesis in liver cancer.[24] In c-myc overexpressing and PTEN deleted murine model of liver cancer, ACSS2 knockout can significantly reduce the incidence of liver cancers.[24] The roles of ACSS2 in pancreatic cancer tumorigenesis and progression remains poorly defined. ACSS2 is the downstream target of sterol regulatory element-binding protein 2 (SREBP2), which was activated when tumor cells exposed to acidic tumor microenvironment.[25] ACSS2 is highly expressed in PanIN lesions and pancreatic cancer tissue, but its role on regulating metabolic reprogramming in pancreatic cancer remains uncharacterized.[12] Management of cachexia remains an unmet need for most gastrointestinal cancers, especially pancreatic cancer. The systematic reprogramming of metabolic profiles drives cancer cachexia to provide nutrients to support tumor growth. [1]

Macropinocytosis is a non-selected protein scavenging process critical for tumor progression, especially for KRAS mutant tumors, such as pancreatic cancer, which is characterized with desmoplasia and nutrient deficiency.[6, 26] KRAS mutation can upregulate macropinocytosis, which provides essential supply of amino acids for tumor growth in nutrient deficient microenvironment. Tumor cells under metabolic stress upregulate macropinocytosis through metabolic reprogramming. For instance, glutamine deficiency upregulates macropinocytosis to maintain amino acid supply in pancreatic cancer.[27] ACSS2 expression in tumor cells was increased when glucose or serum in the culture medium was deficient, indicating tumor cells reprogramed the metabolic profiles to maintain fitness under nutrient deficient microenvironment. We found that nutrient deficient microenvironment can upregulate ACSS2 in pancreatic cancer. We explored the mechanism of ACSS2 increased macropinocytosis in pancreatic cancer and identified a zinc transporter ZIP4 as a downstream target of ACSS2. ZIP4 can promote cancer cachexia, gemcitabine resistance and epithelial-mesenchymal transition in pancreatic cancer.[15, 28–30] We found that ACSS2 upregulates ZIP4 through ETV4 mediated transcriptional activation. Then, we explored how ZIP4 regulates macropinocytosis. Studies showed that pancreatic cancer upregulates macropinocytosis via SDC1, EGFR pathways.[27, 31] To evaluate the role of ACSS2 in mediating macropinocytosis, we analyzed the correlation between ACSS2 and macropinocytosis associated genes. We found that ACSS2 can upregulate macropinocytosis by increasing the expression of macropinocytosis associated genes such as SDC1 and DNM2. Knockdown of ZIP4 can reverse ACSS2 induced macropinocytosis. PI3K-AKT pathway is critical for RAS induced macropinocytosis.[32] We found that ACSS2 can induce the phosphorylation of GSK3β and CREB, which is partially dependent on ZIP4. CREB can bind to the promoter region of SDC1 (CD138). Another study showed that GSK3β

pathway promotes endocytosis by activating dynamin-1.[33] This is consistent to our findings showing that ACSS2 can promotes macropinocytosis. Intriguingly, we found that the impact of ZIP4 downregulation on macropinocytosis is not as substantial as ACSS2 downregulation, indicating additional downstream mediators of ACSS2 may also play important roles on macropinocytosis, which may be independent of ZIP4. Downregulation of ZIP4 have more dramatic effect on pancreatic cancer proliferation than macropinocytosis, suggesting the potential cell autonomous effects of ZIP4 downregulation that go beyond macropinocytosis, such as ZIP4 mediated miR-373 and ENT1 pathways.[16, 21, 29] Together, the evidence above demonstrate that metabolic stress can upregulate ACSS2, which promotes macropinocytosis via ZIP4/CREB/SDC1 pathway to support tumor growth.

On the other side, we found that ACSS2 knockout can attenuate body weight loss, adipose loss and muscle wasting, all of which are characteristics of cancer cachexia. Cancer induced metabolic reprogramming is believed to be the driving force of tissue catabolism and imbalanced energy expenditure in cachexia.[2] Cancer derived circulating factors have garnered substantial attention in the field of cachexia in the past decade, including TGF-β superfamily (Hsp70/90, Activin A, TGF-β, Myostatin, GDF15),[16, 34, 35] TNF superfamily (TNF),[36] IL-6,[37] LIF,[38] etc. These pro-cachexia factors are involved in integrated alterations on metabolism. For example, GDF-15 induced anorexia and lipolysis by interacting with central nervous system and adipose tissue.[34] IL-6 induced cachexia by orchestrating the cross-talk between muscle and adipose tissue.[37] Nonetheless, the molecular mechanism of pancreatic cancer induced cachexia, especially muscle wasting remains poorly understood. Emerging evidence showed that pancreatic cancer cells induced muscle atrophy by secreting TGF-β, IL-6, etc.[16, 37] These cytokines induce muscle atrophy by activating Atrogin-1 (FBXO32) and MuRF1 (TRIM63) mediated muscle fiber degradation.[30] Our study found that ACSS2 knockout cells reduced the levels of several pro-cachexia factors including IL-1A, IL-1B, TGF-β, and TRAIL. Meanwhile, the levels of several anti-cachexia factors were increased in the ACSS2 knockout pancreatic cancer cells, including FGF2 and IL-15. These results indicate ACSS2 can reprogram the metabolic profiles of pancreatic cancer cells to induce cachexia. Among these factors, we are particularly interested in TRAIL (also known as TNFSF10). TRAIL is a member of the TNF superfamily, which is correlated to cachexia in pancreatic cancer.[39] Knockdown of ZIP4 can reverse ACSS2 induced TRAIL expression. Furthermore, we found that TRAIL expression is associated with worse overall survival of patients. Combination of ZIP4 and TRAIL can stratify patients with different prognosis more precisely. We found that ACSS2 can induce phosphorylation of GSK3β at Ser9 and thus inhibits the activity of GSK3β. Emerging evidence showed that macropinocytosis can induce phosphorylation of AKT, which would lead to increased cell proliferation and resistance to mTOR inhibition in KRAS driven pancreatic cancer.[40] Since AKT can induce phosphorylation of GSK3β, the latter of which would upregulate TRAIL, we speculated that macropinocytosis may also promote cancer cachexia. Specifically, in order to meet the high demand of nutrients, tumor cells rewired their metabolic profiles to induce cancer cachexia. The degraded muscle fibers and adipose tissue could provide tumor cells with additional nutrients needed for tumor growth, forming a feedforward loop. Further studies are warranted to address the crosstalk between macropinocytosis and cachexia.

In summary, our study described a previously uncharacterized role of ACSS2 in dominating metabolic reprogramming in pancreatic cancer. ACSS2 increases macropinocytosis to support tumor progression and promotes cancer cachexia to provide nutrients for tumor growth. Specifically, ACSS2 promotes metabolic reprogramming through ETV4/ZIP4 pathway, whereby ZIP4 promotes macropinocytosis via CREB activated SDC1/DNM2 pathway and drives muscle wasting through GSK3β/TRAIL signaling axis, which fuels back the tumor cells to provide additional nutrients to maintain tumor fitness in pancreatic cancer. These results indicate that ACSS2 is an attractive vulnerability for the treatment of cachexia induced by pancreatic cancer.

Supplementary Material

Refer to Web version on PubMed Central for supplementary material.

Funding

This work was supported in part by National Institutes of Health (NIH) grants R01 CA186338, R01 CA203108, R01 CA247234, and the William and Ella Owens Medical Research Foundation (Li), and NIH/National Cancer Institute award P30CA225520.

Abbreviations used in this paper:

ACSS2	Acetyl-coA Synthetase Short-Chain Family Member 2
ZIP4	Solute Carrier Family 39 (Zinc Transporter), Member 4
ETV4	ETS Variant Transcription Factor 4
SDC1	Syndecan 1
DNM2	Dynamin 2
Binding Protein 1	
TRAIL	TNF Superfamily Member 10
MuRF1	Tripartite Motif Containing 63
MHC	Myosin Heavy Chain
BAT	brown adipose tissue
ING	inguinal adipose tissue
EPI	epididymal adipose tissue

References

1. Baracos VE, Martin L, Korc M, et al. Cancer-associated cachexia. Nat Rev Dis Primers 2018;4:17105. [PubMed: 29345251]
2. Argiles JM, Stemmler B, Lopez-Soriano FJ, et al. Inter-tissue communication in cancer cachexia. Nat Rev Endocrinol 2018;15:9–20. [PubMed: 30464312]

3. Huot JR, Pin F, Narasimhan A, et al. ACVR2B antagonism as a countermeasure to multi-organ perturbations in metastatic colorectal cancer cachexia. J Cachexia Sarcopenia Muscle 2020;11:1779–1798. [PubMed: 33200567]
4. Roeland EJ, Bohlke K, Baracos VE, et al. Management of Cancer Cachexia: ASCO Guideline. J Clin Oncol 2020;38:2438–2453. [PubMed: 32432946]
5. Wood LD, Canto MI, Jaffee EM, et al. Pancreatic Cancer: Pathogenesis, Screening, Diagnosis and Treatment. Gastroenterology 2022.
6. Kamphorst JJ, Nofal M, Commisso C, et al. Human pancreatic cancer tumors are nutrient poor and tumor cells actively scavenge extracellular protein. Cancer Res 2015;75:544–53. [PubMed: 25644265]
7. Hosein AN, Brekken RA, Maitra A. Pancreatic cancer stroma: an update on therapeutic targeting strategies. Nat Rev Gastroenterol Hepatol 2020;17:487–505. [PubMed: 32393771]
8. Ramirez C, Hauser AD, Vucic EA, et al. Plasma membrane V-ATPase controls oncogenic RAS-induced macropinocytosis. Nature 2019;576:477–481. [PubMed: 31827278]
9. Schug ZT, Peck B, Jones DT, et al. Acetyl-CoA synthetase 2 promotes acetate utilization and maintains cancer cell growth under metabolic stress. Cancer Cell 2015;27:57–71. [PubMed: 25584894]
10. Mashimo T, Pichumani K, Vemireddy V, et al. Acetate is a bioenergetic substrate for human glioblastoma and brain metastases. Cell 2014;159:1603–14. [PubMed: 25525878]
11. Luong A, Hannah VC, Brown MS, et al. Molecular characterization of human acetyl-CoA synthetase, an enzyme regulated by sterol regulatory element-binding proteins. J Biol Chem 2000;275:26458–66. [PubMed: 10843999]
12. Carrer A, Trefely S, Zhao S, et al. Acetyl-CoA Metabolism Supports Multistep Pancreatic Tumorigenesis. Cancer Discov 2019;9:416–435. [PubMed: 30626590]
13. Slaymaker IM, Gao L, Zetsche B, et al. Rationally engineered Cas9 nucleases with improved specificity. Science 2016;351:84–8. [PubMed: 26628643]
14. Joung J, Konermann S, Gootenberg JS, et al. Genome-scale CRISPR-Cas9 knockout and transcriptional activation screening. Nat Protoc 2017;12:828–863. [PubMed: 28333914]
15. Liu M, Zhang Y, Yang J, et al. Zinc-Dependent Regulation of ZEB1 and YAP1 Coactivation Promotes Epithelial-Mesenchymal Transition Plasticity and Metastasis in Pancreatic Cancer. Gastroenterology 2021;160:1771–1783 e1. [PubMed: 33421513]
16. Shi X, Yang J, Liu M, et al. Circular RNA ANAPC7 Inhibits Tumor Growth and Muscle Wasting Via PHLPP2-AKT-TGF-beta Signaling Axis in Pancreatic Cancer. Gastroenterology 2022;162:2004–2017 e2. [PubMed: 35176309]
17. Zhou Z, Xia G, Xiang Z, et al. A C-X-C Chemokine Receptor Type 2-Dominated Cross-talk between Tumor Cells and Macrophages Drives Gastric Cancer Metastasis. Clin Cancer Res 2019;25:3317–3328. [PubMed: 30796034]
18. Commisso C, Flinn RJ, Bar-Sagi D. Determining the macropinocytic index of cells through a quantitative image-based assay. Nat Protoc 2014;9:182–92. [PubMed: 24385148]
19. Durbin AD, Wang T, Wimalasena VK, et al. EP300 Selectively Controls the Enhancer Landscape of MYCN-Amplified Neuroblastoma. Cancer Discov 2022;12:730–751. [PubMed: 34772733]
20. Mews P, Donahue G, Drake AM, et al. Acetyl-CoA synthetase regulates histone acetylation and hippocampal memory. Nature 2017;546:381–386. [PubMed: 28562591]
21. Zhang Y, Yang J, Cui X, et al. A novel epigenetic CREB-miR-373 axis mediates ZIP4-induced pancreatic cancer growth. EMBO Mol Med 2013;5:1322–34. [PubMed: 23857777]
22. Kim C, Wilcox-Adelman S, Sano Y, et al. Antiinflammatory cAMP signaling and cell migration genes co-opted by the anthrax bacillus. Proc Natl Acad Sci U S A 2008;105:6150–5. [PubMed: 18427110]
23. Li X, Yu W, Qian X, et al. Nucleus-Translocated ACSS2 Promotes Gene Transcription for Lysosomal Biogenesis and Autophagy. Mol Cell 2017;66:684–697 e9. [PubMed: 28552616]
24. Comerford SA, Huang Z, Du X, et al. Acetate Dependence of Tumors. Cell 2014;159:1591–1602. [PubMed: 25525877]

25. Kondo A, Yamamoto S, Nakaki R, et al. Extracellular Acidic pH Activates the Sterol Regulatory Element-Binding Protein 2 to Promote Tumor Progression. Cell Rep 2017;18:2228–2242. [PubMed: 28249167]
26. Su H, Yang F, Fu R, et al. Cancer cells escape autophagy inhibition via NRF2-induced macropinocytosis. Cancer Cell 2021;39:678–693 e11. [PubMed: 33740421]
27. Lee SW, Zhang Y, Jung M, et al. EGFR-Pak Signaling Selectively Regulates Glutamine Deprivation-Induced Macropinocytosis. Dev Cell 2019;50:381–392 e5. [PubMed: 31257175]
28. Liu M, Yang J, Zhang Y, et al. ZIP4 Promotes Pancreatic Cancer Progression by Repressing ZO-1 and Claudin-1 through a ZEB1-Dependent Transcriptional Mechanism. Clin Cancer Res 2018;24:3186–3196. [PubMed: 29615456]
29. Liu M, Zhang Y, Yang J, et al. ZIP4 Increases Expression of Transcription Factor ZEB1 to Promote Integrin alpha3beta1 Signaling and Inhibit Expression of the Gemcitabine Transporter ENT1 in Pancreatic Cancer Cells. Gastroenterology 2020;158:679–692 e1. [PubMed: 31711924]
30. Yang J, Zhang Z, Zhang Y, et al. ZIP4 Promotes Muscle Wasting and Cachexia in Mice With Orthotopic Pancreatic Tumors by Stimulating RAB27B-Regulated Release of Extracellular Vesicles From Cancer Cells. Gastroenterology 2019;156:722–734 e6. [PubMed: 30342032]
31. Yao W, Rose JL, Wang W, et al. Syndecan 1 is a critical mediator of macropinocytosis in pancreatic cancer. Nature 2019;568:410–414. [PubMed: 30918400]
32. Amyere M, Payrastre B, Krause U, et al. Constitutive macropinocytosis in oncogene-transformed fibroblasts depends on sequential permanent activation of phosphoinositide 3-kinase and phospholipase C. Mol Biol Cell 2000;11:3453–67. [PubMed: 11029048]
33. Reis CR, Chen PH, Srinivasan S, et al. Crosstalk between Akt/GSK3beta signaling and dynamin-1 regulates clathrin-mediated endocytosis. EMBO J 2015;34:2132–46. [PubMed: 26139537]
34. Suriben R, Chen M, Higbee J, et al. Antibody-mediated inhibition of GDF15-GFRAL activity reverses cancer cachexia in mice. Nat Med 2020;26:1264–1270. [PubMed: 32661391]
35. Loumaye A, de Barsy M, Nachit M, et al. Circulating Activin A predicts survival in cancer patients. J Cachexia Sarcopenia Muscle 2017;8:768–777. [PubMed: 28712119]
36. Johnston AJ, Murphy KT, Jenkinson L, et al. Targeting of Fn14 Prevents Cancer-Induced Cachexia and Prolongs Survival. Cell 2015;162:1365–78. [PubMed: 26359988]
37. Rupert JE, Narasimhan A, Jengelley DHA, et al. Tumor-derived IL-6 and trans-signaling among tumor, fat, and muscle mediate pancreatic cancer cachexia. J Exp Med 2021;218.
38. Kandarian SC, Nosacka RL, Delitto AE, et al. Tumour-derived leukaemia inhibitory factor is a major driver of cancer cachexia and morbidity in C26 tumour-bearing mice. J Cachexia Sarcopenia Muscle 2018;9:1109–1120. [PubMed: 30270531]
39. Freire PP, Fernandez GJ, de Moraes D, et al. The expression landscape of cachexia-inducing factors in human cancers. J Cachexia Sarcopenia Muscle 2020;11:947–961. [PubMed: 32125790]
40. Michalopoulou E, Auciello FR, Bulusu V, et al. Macropinocytosis Renders a Subset of Pancreatic Tumor Cells Resistant to mTOR Inhibition. Cell Rep 2020;30:2729–2742 e4. [PubMed: 32101748]

What You Need to Know

BACKGROUND AND CONTEXT

Cachexia and metabolic reprogramming are two hallmarks of pancreatic cancer. ACSS2 is an acetyl-coA synthetase that contributes to lipid synthesis and epigenetic reprogramming. We demonstrate that ACSS2 potentiates macropinocytosis and muscle wasting through metabolic reprogramming in pancreatic cancer.

NEW FINDINGS

ACSS2 promotes metabolic reprogramming through ETV4/ZIP4 pathway, whereby ZIP4 promotes macropinocytosis via SDC1/DNM2 and drives muscle wasting through GSK3β/TRAIL pathway, which in turn provides additional nutrients for macropinocytosis in pancreatic cancer.

LIMITATIONS

This study was performed in cell lines and mouse models. Further studies are needed to validate in patients.

IMPACT

This study identifies ACSS2 as a key regulator that potentiates macropinocytosis and muscle wasting through metabolic reprogramming, thus representing an attractive therapeutic target to attenuate cachexia in pancreatic cancer.

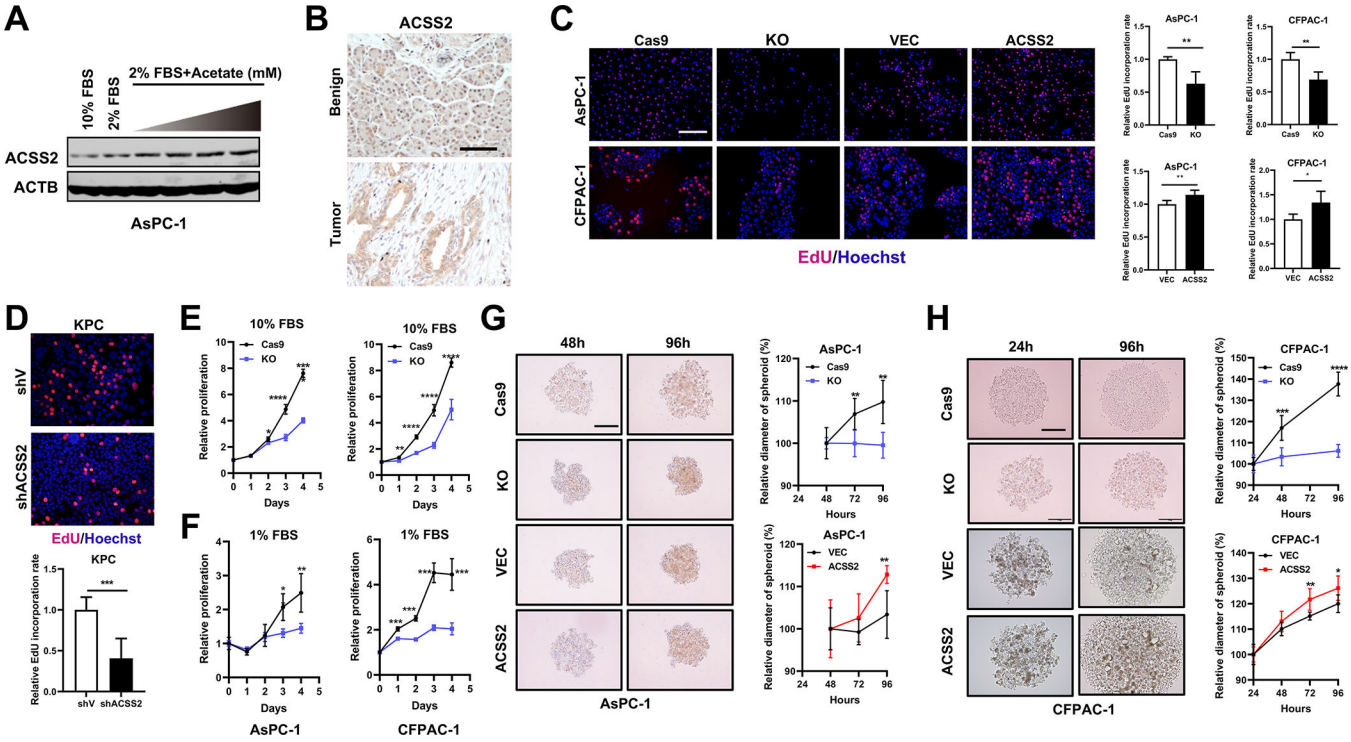

Figure 1.

Metabolic stress induces ACSS2 expression and promotes cell proliferation. (*A*) ACSS2 expression of AsPC-1 cells treated with complete medium, 2% serum medium, and 2% serum medium supplemented with gradient concentration of sodium acetate for 72 hours. (*B*) ACSS2 expression in human pancreatic cancer tissues and benign pancreas tissues. Scale bar is 50 μm. (*C*) DNA synthesis rate was assessed by EdU incorporation assay in ACSS2 knockout or overexpression cell lines. Scale bar is 100 μm. (*D*) DNA synthesis rate was assessed by EdU incorporation assay in ACSS2 knockdown KPC cells. Scale bar is 50 μm. (*E-F*) Cell proliferation was assessed by MTT assay in ACSS2 knockout cell lines in complete medium or medium with 1% FBS. (*G-H*) Relative size of spheroids established from ACSS2 knockout or overexpression cell lines. Scale bar is 200 μm. (* $P<0.05$, ** $P<0.01$, *** $P<0.001$, **** $P<0.0001$).

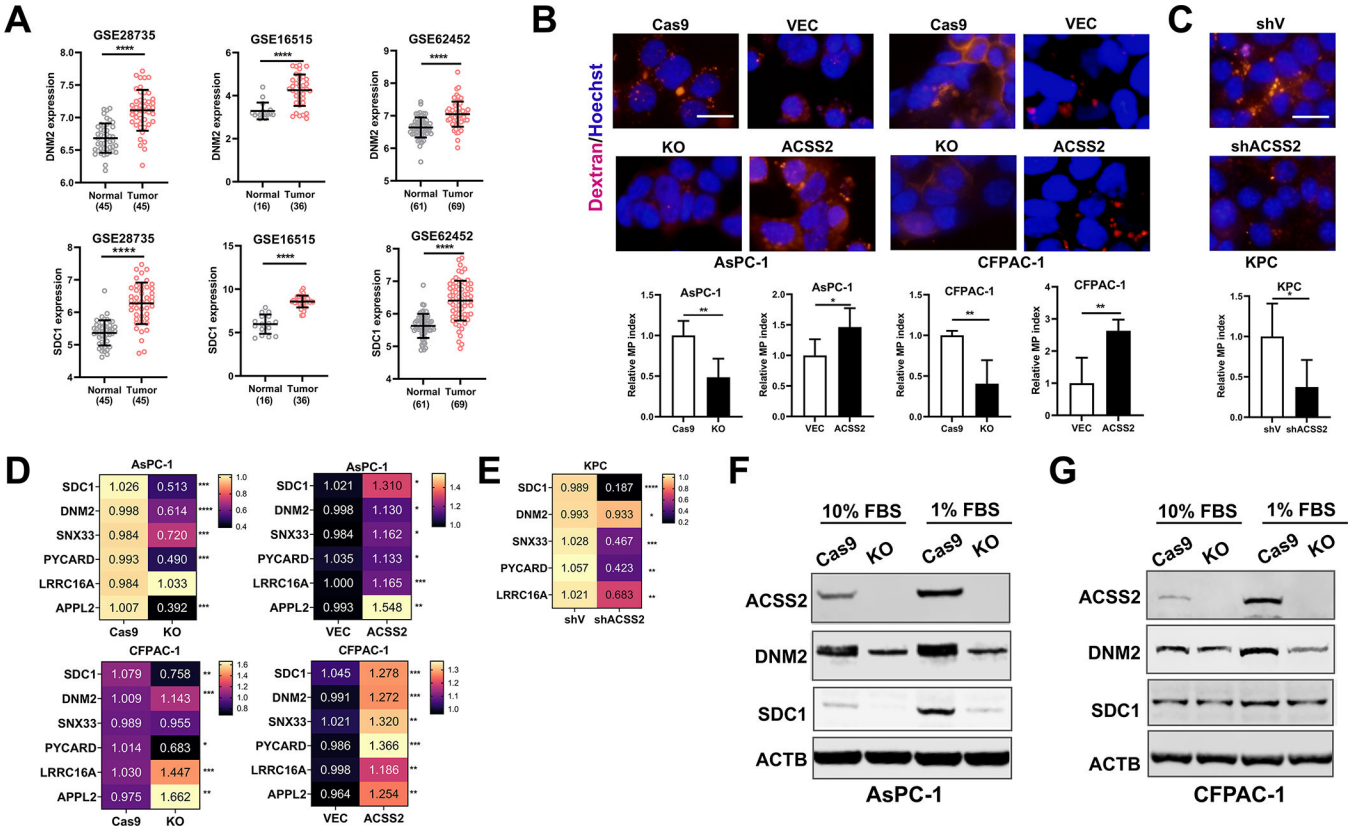

Figure 2.

ACSS2 upregulates macropinocytosis in pancreatic cancer progression. (*A*) Expression level of DNM2 and SDC1 in pancreatic cancer cohorts. (*B*) Dextran uptake assay to assess macropinocytosis index in ACSS2 knockout and overexpression human cell lines. Scale bar is 10 μm. (*C*) Dextran uptake assay to assess macropinocytosis index in ACSS2 knockdown KPC cells. Scale bar is 10 μm. (*D-E*) The mRNA level of macropinocytosis associated genes in ACSS2 knockout and overexpression human cell lines and in ACSS2 knockdown KPC cell line. (*F-G*) The protein level of macropinocytosis associated genes in ACSS2 knockout cell lines cultured in normal condition or stress condition.

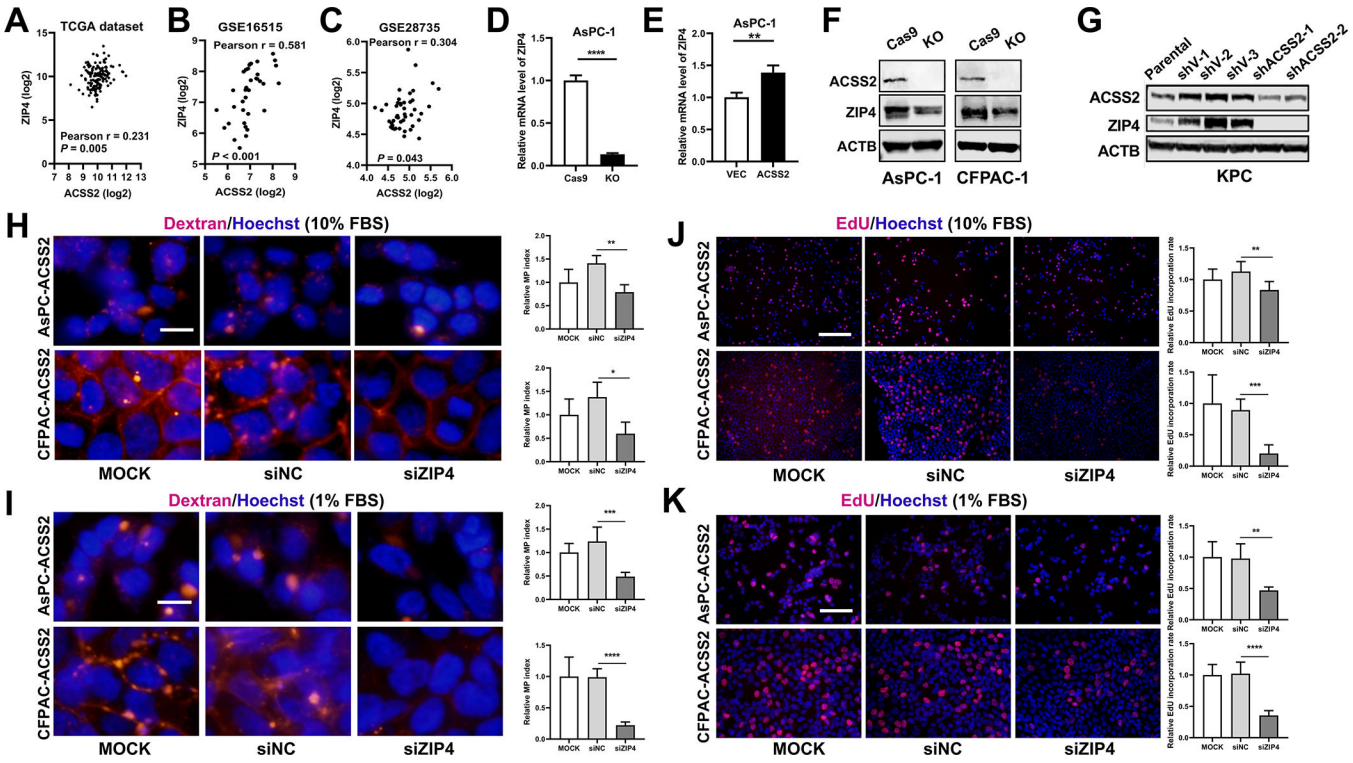

Figure 3.

ACSS2 promotes macropinocytosis through ZIP4. (*A-C*) Correlation between ACSS2 and ZIP4 expression in TCGA cohort, GSE16515 cohort and GSE28735 cohort. (*D-E*) mRNA level of ZIP4 in ACSS2 knockout or overexpression cell lines. (*F*) Protein level of ZIP4 in ACSS2 knockout cell lines. (*G*) Protein levels of ZIP4 in ACSS2 knockdown KPC cells. (*H-I*) Dextran uptake assay to assess macropinocytosis index in ACSS2 overexpression cell lines with ZIP4 knockdown in 10% FBS or 1% FBS. Scale bar is 10 μm. (*J-K*) DNA synthesis rate was assessed by EdU incorporation assay in ACSS2 overexpression cell lines transfected with siNC or siZIP4 siRNA under metabolic stress. Scale bar is 100 μm and 50 μm respectively. (* P<0.05, ** P<0.01, *** P<0.001, **** P<0.0001).

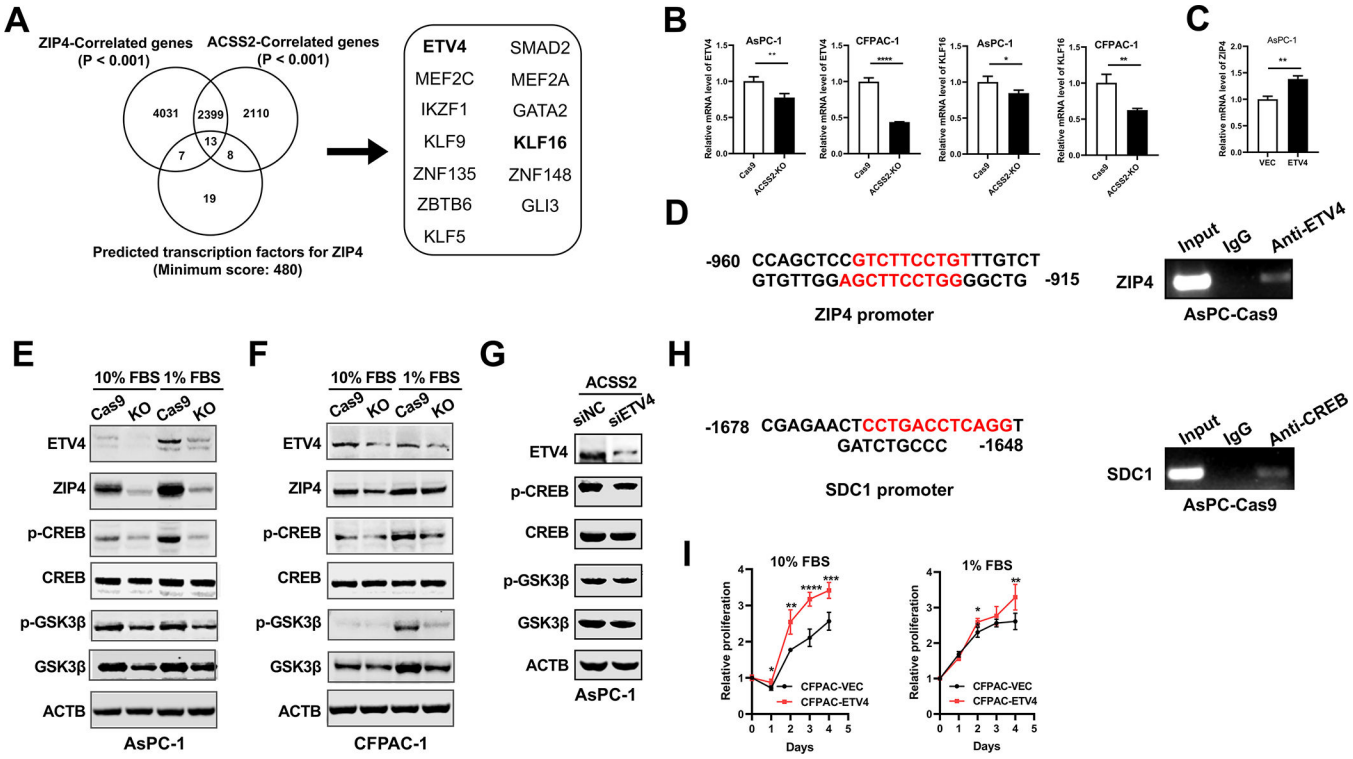

Figure 4.

ACSS2 promotes macropinocytosis through ETV4/ZIP4/CREB pathway. (*A*) Venn Diagram showing the candidates of transcription factors for ZIP4. (*B*) mRNA level of ETV4 and KLF16 in ACSS2 knockout cell lines. (*C*) mRNA level of ZIP4 in ETV4 overexpression AsPC-1 cells. (*D*) Predicted binding site of ETV4 on ZIP4 promoter region (left panel). ChIP assay to evaluate ETV4 binds to the promoter region of ZIP4 (right panel). (*E-F*) Protein level of ETV4, ZIP4, p-GSK3β, total-GSK3β, p-CREB, total-CREB in ACSS2 knockout cell lines in 10% FBS or 1% FBS. (*G*) Protein level of ETV4, p-GSK3β, total-GSK3β, p-CREB and total-CREB in ETV4 knockdown and ACSS2 overexpression cell lines. (*H*) Predicted binding site of CREB on SDC1 promoter region (left panel). ChIP assay to evaluate CREB binds to the promoter region of SDC1 (right panel). (*I*) Cell proliferation was assessed by MTT assay in ETV4 overexpression cell lines in 10% FBS or 1% FBS. (* $P<0.05$, ** $P<0.01$, *** $P<0.001$, **** $P<0.0001$).

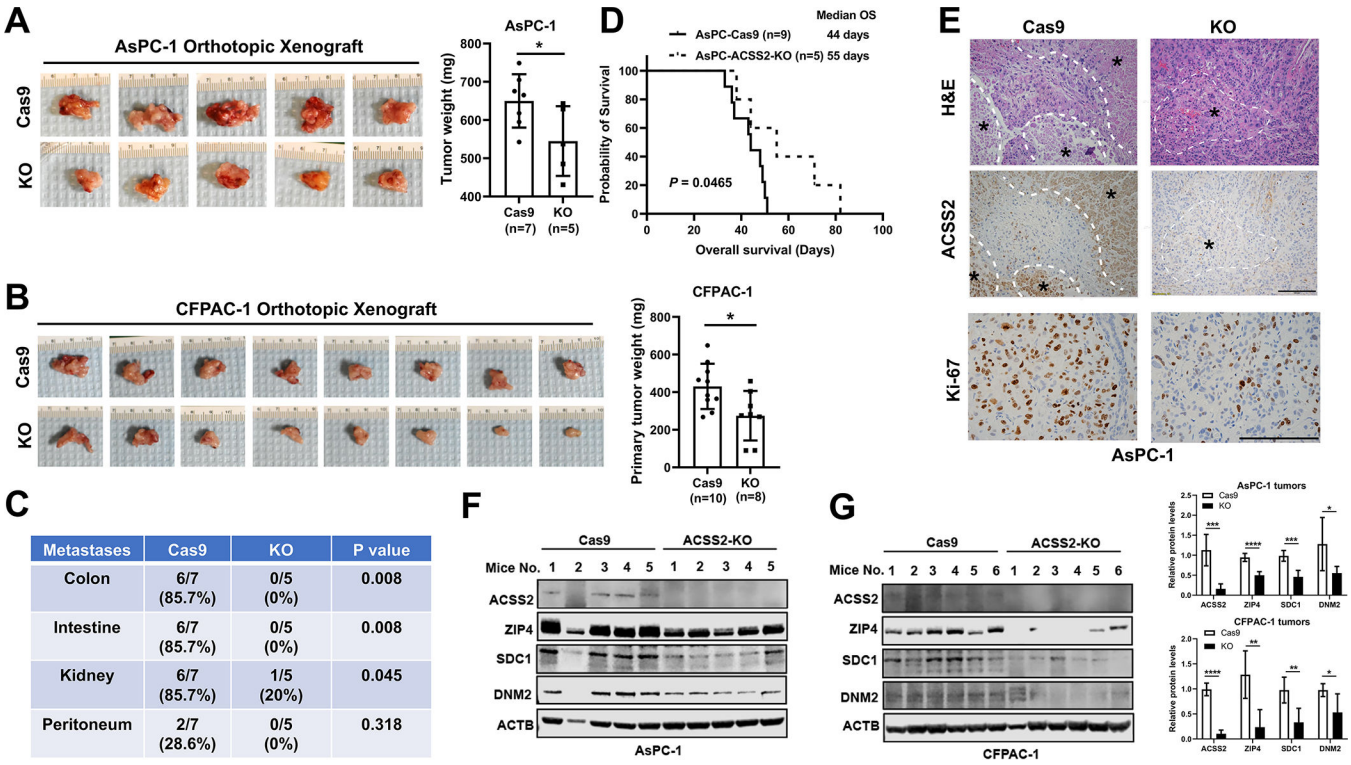

Metastases	Cas9	KO	P value
Colon	6/7 (85.7%)	0/5 (0%)	0.008
Intestine	6/7 (85.7%)	0/5 (0%)	0.008
Kidney	6/7 (85.7%)	1/5 (20%)	0.045
Peritoneum	2/7 (28.6%)	0/5 (0%)	0.318

Figure 5.

ACSS2 knockout suppresses tumor growth in orthotopic xenograft mouse models. (*A-B*) Representative images of tumor mass and tumor weight in pancreatic cancer orthotopic xenograft mouse models. (*C*) Summary of metastases in mice xenografted with AsPC-Cas9 or AsPC-ACSS2-KO tumors. (*D*) Overall survival of mice xenografted with AsPC-Cas9 or AsPC-ACSS2-KO tumors. (*E*) Representative images of H&E staining, ACSS2 and Ki-67 expression in the xenograft tumor tissue. The areas marked with "*" indicated areas with metabolic stress. Scale bar is 100 μm. (*F-G*) Expression of ACSS2, ZIP4 and macropinocytosis associated genes (SDC1, DNM2) were evaluated in mice tumor tissue. (* $P<0.05$, ** $P<0.01$, *** $P<0.001$, **** $P<0.0001$).

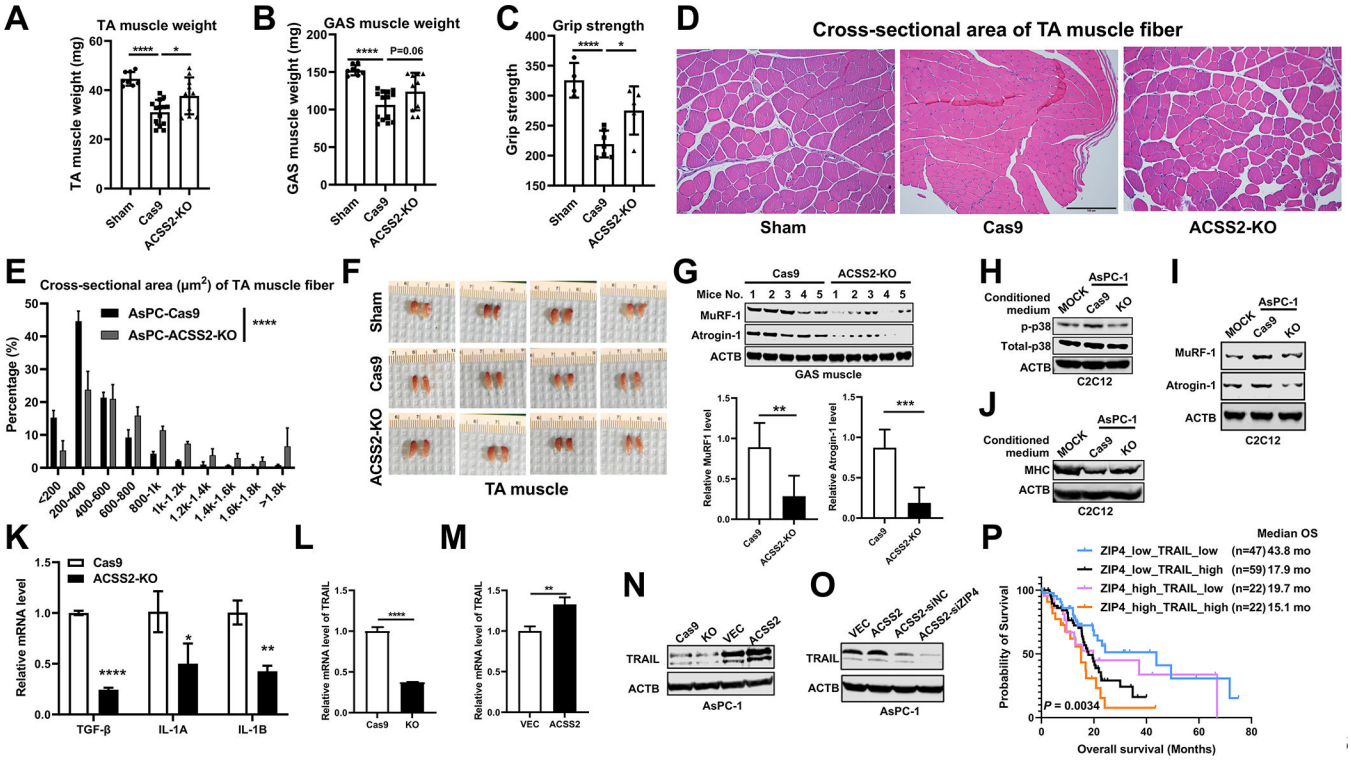

Figure 6.

ACSS2 promotes muscle wasting through GSK3B/TRAIL pathway. (*A-B*) Statistics of mouse tibialis anterior (TA) muscle weight and gastrocnemius (GAS) muscle weight. (*C*) Muscle grip strength of the mice. (*D*) Representative images of H&E staining of cross-sectional area of TA muscle fiber in SHAM, AsPC-Cas9 and AsPC-ACSS2-KO groups. Scale bar is 100 μm. (*E*) Statistics result of cross-sectional area of TA muscle fiber in Sham, AsPC-Cas9 and AsPC-ACSS2-KO tumor. (*F*) Representative images of TA muscle in xenograft mouse models. (*G*) Protein levels of Atrogin-1 and MuRF1 in mice GAS muscle tissue. (*H-J*) Protein levels of p-p38, total-p38, MuRF-1, Atrogin-1, MHC in C2C12 myotubes treated with conditioned medium from AsPC-Cas9 or AsPC-ACSS2-KO cell lines. (*K*) mRNA level of pro-cachexia markers in ACSS2 knockout or overexpression cell lines. (*L-M*) Protein level of TRAIL in ACSS2 knockout and overexpression AsPC-1 cells. (*N-O*) Protein level of TRAIL in ACSS2 vector or ACSS2 overexpression AsPC-1 cells transfected with siNC or siZIP4 siRNA. (*P*) Survival analysis of pancreatic cancer in TCGA cohort (n=150) based on TRAIL and ZIP4 expression. (* $P<0.05$, ** $P<0.01$, *** $P<0.001$, **** $P<0.0001$).

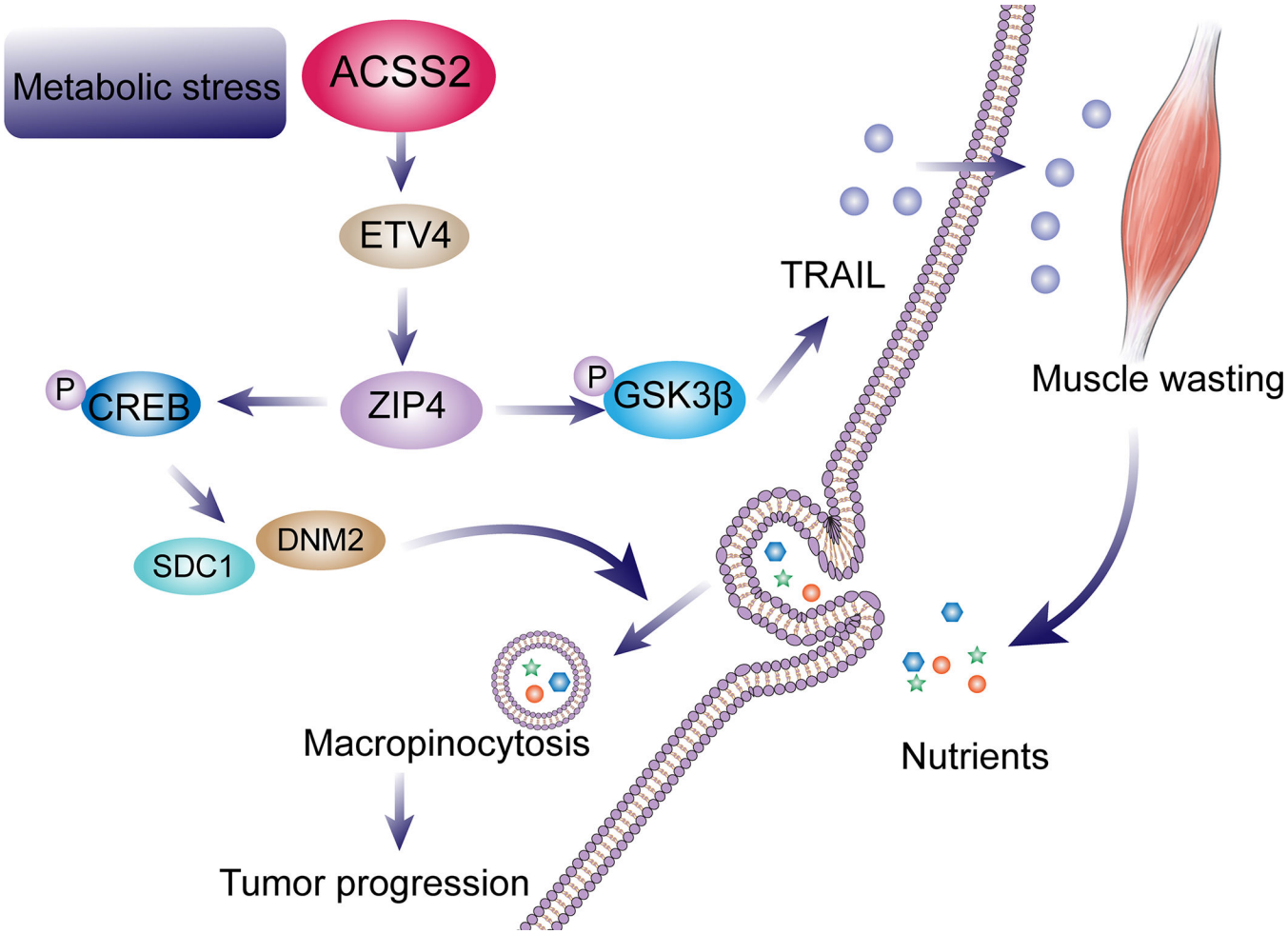

Figure 7.

Schematic diagram of ACSS2 mediated macropinocytosis and cancer cachexia in pancreatic cancer. ACSS2 promotes metabolic reprogramming through ETV4/ZIP4 pathway, whereby ZIP4 promotes macropinocytosis via SDC1/DNM2 and drives muscle wasting through GSK3ß/TRAIL axis, which in turn provides additional nutrients for macropinocytosis in pancreatic cancer.